

Assessment of two quasi-static approaches to mimic repeated impact response and damage behaviour of CFRP laminates

Huo, L.; Verstraeten, A.J.M.; Alderliesten, R.C.

DOI

[10.1016/j.cja.2023.01.015](https://doi.org/10.1016/j.cja.2023.01.015)

Publication date

2023

Document Version

Final published version

Published in

Chinese Journal of Aeronautics

Citation (APA)

Huo, L., Verstraeten, A. J. M., & Alderliesten, R. C. (2023). Assessment of two quasi-static approaches to mimic repeated impact response and damage behaviour of CFRP laminates. *Chinese Journal of Aeronautics*, 36(8), 101-114. <https://doi.org/10.1016/j.cja.2023.01.015>

Important note

To cite this publication, please use the final published version (if applicable).
Please check the document version above.

Copyright

Other than for strictly personal use, it is not permitted to download, forward or distribute the text or part of it, without the consent of the author(s) and/or copyright holder(s), unless the work is under an open content license such as Creative Commons.

Takedown policy

Please contact us and provide details if you believe this document breaches copyrights.
We will remove access to the work immediately and investigate your claim.



Chinese Society of Aeronautics and Astronautics
& Beihang University

Chinese Journal of Aeronautics

cja@buaa.edu.cn
www.sciencedirect.com



Assessment of two quasi-static approaches to mimic repeated impact response and damage behaviour of CFRP laminates

Lubin HUO *, Dries VERSTRAETEN, René ALDERLIESTEN

Structural Integrity & Composites Group, Faculty of Aerospace Engineering, Delft University of Technology, P.O. Box 5058, 2600 GB Delft, the Netherlands

Received 30 June 2022; revised 28 July 2022; accepted 18 October 2022
Available online 3 February 2023

KEYWORDS

Composite laminates;
Damage detection;
Damage characterization;
Low-velocity impact;
Quasi-static indentation;
Thermoset composites

Abstract Full impact damage tolerance assessment requires the ability to properly mimic the repeated impact response and damage behaviour of composite materials using quasi-static approximations. To this aim, this paper reports an experimental investigation evaluating two quasi-static methods for mimicking repeated impact response and damage behaviour of Carbon Fibre Reinforced Polymer (CFRP) composite laminates. In this study, an 8.45-J single impact was repeated 225 times and mimicked with 225 times 6.51-J quasi-static (energy equivalent) indentations and with 225 quasi-static (force equivalent) indentations following the recorded impact peak force variation. Results show that the loading rate and the inertial effect are the two major factors affecting the responses of the composite laminates under out-of-plane concentrated loading. Both the energy- and force-equivalent quasi-static indentations failed to reproduce the impact responses greatly associated with high loading rate and inertial effect. The force-equivalent quasi-static indentations were performed in a semi-automatic way and induced damage states more similar to those of the repeated impacts than those of the energy-equivalent quasi-static indentations, whereas the latter can be better automated and has better reproducibility compared to that of the repeated impact responses, as it is less dependent on high loading rate and inertial effect.

© 2023 Production and hosting by Elsevier Ltd. on behalf of Chinese Society of Aeronautics and Astronautics. This is an open access article under the CC BY-NC-ND license (<http://creativecommons.org/licenses/by-nc-nd/4.0/>).

1. Introduction

Carbon Fibre Reinforced Polymer (CFRP) composites are widely used these days in various engineering applications for higher strength-to-mass and stiffness-to-mass ratios than those of their metallic counterparts. In the aviation industry, both Boeing and Airbus have developed modern commercial aircraft, B787 and A350, respectively, that are made of carbon fibre-reinforced composites accounting for approximately 50%

* Corresponding author.

E-mail address: L.Huo@tudelft.nl (L. HUO).

Peer review under responsibility of Editorial Committee of CJA.



Production and hosting by Elsevier

of their total mass.^{1,2} However, a great weakness of carbon fibre-reinforced composites is that they are generally vulnerable to out-of-plane impact loading, due to the lack of through-thickness reinforcement.³ In particular, Barely Visible Impact Damage (BVID) can be created by out-of-plane impact loading and contributes to losses of stiffness and strength in CFRP laminates.⁴ With the brittle nature of carbon fibre and polymer matrix, opposite to conventional metallic materials,⁵ CFRP composites have the ability to elastically recover to their original states. If there are no visible external damages, such as local permanent dent, surface matrix cracks, and splitting between fibres, impact damages remain undetectable. That is, BVID is often seen as a hidden menace.⁵ A full understanding of the damage behaviours and mechanisms of CFRP composite materials can help designers optimize their design strategies, thereby improving the applicability of CFRP composite structures.

Therefore, extensive studies have been carried out to characterize damage behaviours and reveal damage mechanisms of impacted composite materials/structures,^{6–9} especially for investigations of damage formations in composite laminates caused by repeated out-of-plane impacts (i.e., multiple independent out-of-plane impacts successively applied to the centre of a composite panel).^{10–12} For a composite plate that is repeatedly impacted at one single location, even though the damage increments caused by every single impact may be small, the continuous accumulation of such minor damages can ultimately destroy its integrity.¹³ However, the rate of damage accumulation is determined by a combination of several factors, such as stiffness and strength of composite targets, material properties of impactors, and impact energies. It may need thousands of impacts before sufficient data to support the damage analyses of a repeatedly impacted composite laminate can be acquired. An automated implementation of thousands of impacts is really a challenge for common impact test devices, such as a drop-weight tower¹⁴ and a Charpy impact test device.¹⁵

Because literature has shown that single impacts can be approximated with quasi-static indentation under certain conditions in terms of the similarity of the final damage state,^{16–19} it is not unreasonable to assume that repeated impacts can also be represented by repeated quasi-static indentations. More importantly, what has been known is that repeated quasi-static indentations tests can be automated with state-of-art universal material testing machines, similarly to mechanical fatigue tests, while avoiding negative effects associated with dynamic vibrations. The aim of this work is to assess the feasibility of quasi-static solutions to yield similarities in repeated impact responses and damage behaviours of CFRP composites.

To that end, repeated drop-weight impacts and two types of repeated quasi-static indentations were applied to the centres of fully clamped CFRP laminates. The impact responses of the impacted and indented laminates were characterized and compared based on recorded force–displacement curves and peak force variations. For comparisons of damage states, a combination of non-destructive damage detection techniques (i.e., 3D surface measurement and ultrasonic C-scan) and cross-sectional damage analysis were performed.

2. Background

Composite laminates subjected to either high- or low-velocity impacts behave distinctively differently. For example, Cantwell

and Morton⁹ have shown that deformations of composite laminates under high-velocity impacts are generally localized and restricted to the contact area, while low-velocity impacts cause global deformations, which, in turn, leads to low-velocity impact responses that are generally highly geometry-dependent. In addition, the effects of stress waves on damage formation associated with high-velocity impacts are also more pronounced than those with low-velocity impacts.^{20,21} Due to these factors, high-velocity impacts usually cannot be approximated by quasi-static indentations. On the contrary, relevant studies^{17–19,21–26} have shown that, with the same boundary conditions, low-velocity impacts can be equivalent to quasi-static indentations, because both loading conditions on the same composite panel create comparable damage states. As a matter of fact, as suggested by Castellano et al.,²⁷ owing to that the implementation of low-velocity impact tests is relatively difficult and expensive, and impact test results are generally complex and largely scattered, many researchers have sought quasi-static solutions or approximations to assess the low-velocity impact damage behaviours of composites.^{21,23,28–29} A typical application of quasi-static indentation has been presented by Wagih et al.,¹⁶ who conducted a series of quasi-static indentations to elucidate the damage sequence of composite laminates subjected to low-velocity impacts. Lammerant and Verpoest³⁰ attempted to clarify the interaction between the impact matrix crack and delamination by using quasi-static indentations. Lee and Zahuta²³ tried to visualize the impact damage growth process as the impact force surged to its maximum value through the growth of the corresponding indentation damages.

Those studies used quasi-static indentations to investigate the damage behaviours and mechanisms of composite materials subjected to low-velocity impacts, but the question that remains to be answered is how to properly define such an equivalence. To clearly answer this question, it is necessary to find out common damage metrics between low-velocity impacts and quasi-static indentations. The common damage metrics here refer to the indices directly associated with the initiation and propagation of various impact and indentation damages. In an impact test, the force–time curve can be directly recorded (a typical force–time curve is shown in Fig. 1(a)), and such an impact force history can convey vital information relevant to damage initiation and growth.²³ A distinctive parameter of the force–time curve is the peak force, denoted as F_{\max} in Fig. 1(a), which is used as an important damage metric,^{31–33} where Liu et al.^{31,34} even suggested that there is a maximum F_{\max} for any laminate. When the impact peak force is below this maximum value, the impact induces only minor damages such as permanent dent and local matrix cracking. Above that maximum value, significant delaminations occur. From the perspective of impact energy, the energies related to damage initiation and propagation can be separately represented by the energies before and after the maximum value of F_{\max} . Note that for an impact, the energy–time curve can be indirectly obtained by numerically integrating the force–time curve, which is shown in Fig. 1(b). The rebound and absorbed energies are separately referred to as the energies associated with the elastic deformations of the impact target and those dissipated due to damages, plastic deformations, dynamic vibrations, etc. In the critical impact case mentioned by Liu, where F_{\max} is just equal to its maximum value, the impact energies obtained before and after F_{\max}

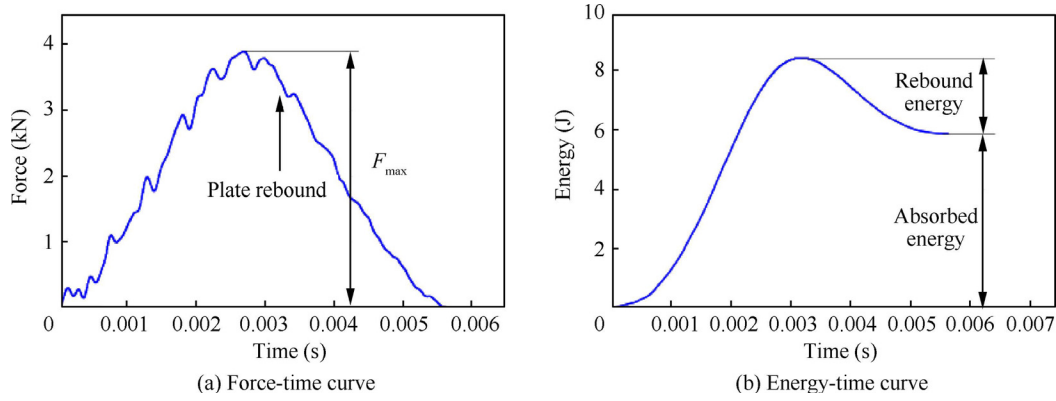


Fig. 1 Typical low-velocity impact force-time and energy-time curves.

are suggested as damage initiation and propagation energies, respectively. The peak force and the energy parameter corresponding to the peak force could be used to establish equivalence between a low-velocity impact and a quasi-static indentation.

Lagace et al.¹⁸ adopted the peak force as a metric to link a low-velocity impact and a quasi-static indentation. They assumed that the peak force is a key factor in controlling damage formations. In their study, low-velocity impacts were first performed on composite laminates, and the corresponding peak forces were recorded during the tests. Subsequently, the same other laminates with identical boundary conditions were indented up to the recorded impact peak forces. In contrast, Kaczmarek and Maison²¹ employed energy as an equivalent metric, and they believed that similar impact and indentation energies could induce a similar final damage status in composites. Therefore, they indented the composite laminates first, and then calculated the indentation energy by numerically integrating the indentation force-deflection curve. Afterwards, they impacted other composite specimens through an instrumented impact tower and equalled the gravitational energy of the impactor with the calculated indentation energy by adjusting the impactor to a certain height before the impact.

Since the energy similitude adopted by Kaczmarek and Maison ignored the energies dissipated by frictions and dynamic vibrations, which instead should be well considered as suggested by Sjoblom et al.,²⁴ the peak force similitude proposed by Lagace et al. is more reasonable. Therefore, for a single impact and indentation, the impact and indentation energies can only be considered equivalent if they induce similar peak forces in the same composite targets with comparable loading conditions, and this relationship can be formulated as

$$(E_{\text{indentation}})_{\text{single}} \sim (E_{\text{impact}})_{\text{single}}, \text{ as long as } (F_{\text{max, indentation}})_{\text{single}} = (F_{\text{max, impact}})_{\text{single}} \quad (1)$$

where $(E_{\text{indentation}})_{\text{single}}$ and $(E_{\text{impact}})_{\text{single}}$ are the single indentation and impact energies, respectively, while $(F_{\text{max, indentation}})_{\text{single}}$ and $(F_{\text{max, impact}})_{\text{single}}$ are the single peak indentation and impact forces.

For repeated impacts, even though the impact energy is identical for each impact, the associated maximum impact force of each impact is not exactly the same due to the damage-induced material property degradation³⁵ and the dynamic vibration of the impact system.¹¹ That is, in the case

of repeated impacts, the impact peak forces and the impact energies are not in a one-to-one correlation. Following exactly the same peak force variation by using repeated quasi-static indentations seems a more logical way to mimic the repeated impact response and damage behaviour than the energy similitude. However, a significant compromise has to be made to use this approach, because the indentation force must be adjusted manually each time according to the impact force variation, which certainly undermines the pursuit of automation.

To overcome this issue, in this study, CFRP laminates were first Repeatedly Impacted (RI) at their centres with the same applied impact energy for each single impact, with the impact peak forces were recorded. Then, two quasi-static indentation methods were employed, and their abilities to mimic the impact responses and damage behaviours of the RI specimens were evaluated. The first one was called Repeated Force equivalent Quasi-Static Indentations (RF-QSI), which exactly followed the same impact peak force variation, i.e.,

$$(F_{\text{max, indentation}})_n = (F_{\text{max, impact}})_n \quad (2)$$

where $(F_{\text{max, indentation}})_n$ and $(F_{\text{max, impact}})_n$ are the peak forces of the n^{th} indentation and impact, respectively.

The second quasi-static method maintained a constant indentation energy that was equivalent to the single impact energy until the indentation test was completed, and thus was named Repeated Energy equivalent Quasi-Static Indentations (RE-QSI). The energies involved in the RE-QSI method have a relationship with the single impact energy as

$$(E_{\text{indentation}})_n \sim (E_{\text{impact}})_{\text{single}} \quad (3)$$

where $(E_{\text{indentation}})_n$ is the indentation energy for the n^{th} indentation, and $(E_{\text{impact}})_{\text{single}}$ is the same as that defined in Eq. (1).

Another major difference between those two quasi-static approaches is that the RE-QSI can be automated after the initial setup on a testing machine, whereas for the RF-QSI, the terminal force for each indentation needs to be manually adjusted according to the recorded impact peak force variation.

3. Experimental details

3.1. Fabrication of specimens

In this study, rectangular CFRP specimens were used with dimensions of 150 mm × 300 mm, a nominal thickness of

2.5 mm, and a quasi-isotropic layup of $[45/0/-45/90]_{2s}$, in which the 0° fibre direction was aligned with the short edge of the specimen. These specimens were cut from a 1000 mm \times 1000 mm \times 2.5 mm hand layup square panel made of carbon/epoxy prepreg M30SC/DT10 supplied by Delta-Tech S.p.a. This CFRP panel was put into an autoclave and cured for 90 mins with a temperature of 120°C and a pressure of 6 bar according to the manufacturer specifications. Finally, ultrasonic C-scanning was performed on all specimens, and those without defects were used for testing.

3.2. Test fixture

ASTM standards D6264-98³⁶ and D7136M-15³⁷ each separately recommend a test fixture for impact and quasi-static indentation tests. With these standard fixtures and test approaches, the damage resistances of various composite materials can be compared. However, the geometrical configurations of these two fixtures for impact and indentation tests are totally different, which, in turn, makes impact and indentation damage behaviours incomparable. To keep the boundary conditions of the impact and indentation specimens consistent, a new test fixture was designed, which is shown in Fig. 2. With this fixture, the short edges of a specimen are bolted, while the long edges are clamped by friction. An approximate four-side clamping boundary condition can thus be provided by this fixture.

3.3. Repeated impact test

The RI test was performed with a drop-weight tower that is shown in Fig. 3(a), in which 225 impacts (the number of impacts was limited by the reality of operating the machine manually) with a constant impact energy of 8.45 J were successively applied vertically to the geometric centre of the specimen through a steel hemispherical impactor. The choice of 8.45 J as the impact energy is based on the pre-experimental results that, under this energy level, the corresponding single impact can be approximated using a quasi-static indentation in terms of damage formed. The impactor has a diameter of 30 mm and was mounted on a steel mass with their total mass up to 2.91 kg. For each impact, the impactor was dropped from a fixed height so that a velocity of 2.41 m/s (± 0.03 m/s) could be achieved at the moment of contact with the front surface of the specimen, theoretically delivering a constant impact energy of 8.45 J. This instant velocity was measured by a velocity sensor placed close to the specimen's front surface (see Fig. 3(a)).

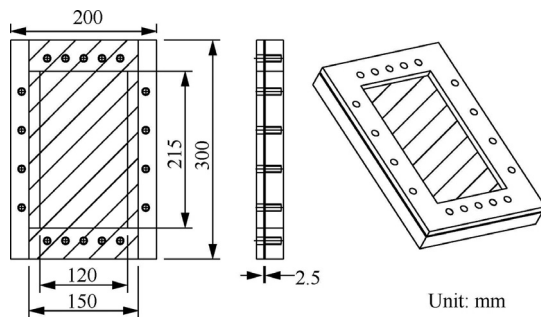


Fig. 2 Test fixture, test specimen clamped in indicated by the hatched area.

After each impact, the rebounded impactor was captured automatically by a capture device to avoid an unexpected secondary impact. Furthermore, a force transducer was adopted to record the contact force history of each impact with an acquisition frequency of 700 kHz.

3.4. Repeated quasi-static indentation test

A Zwick Roell 20-kN servo-hydraulic universal material testing machine, as shown in Fig. 3(b), was employed to conduct the repeated quasi-static indentation tests. Like the repeated impacts, the repeated indentations were also applied to the centre of the fully clamped specimens through a steel indenter with an identical hemispherical shape to that of the impactor, and the indentation rate was 3 mm/min. The force–deflection curve of the composite specimen for each indentation was directly recorded by a force and displacement transducer.

More specifically, the RE-QSI consisted of 225 indentations with an identical energy of 6.51 J. The indentation energy of 6.51 J is considered equivalent to the single impact energy of 8.45 J, as they induced similar peak forces in the composite laminates as illustrated in Eq. (1) and similar final damage statuses as the pre-experimental results suggested. Similarly, the RF-QSI comprised 225 indentations, and the peak force reached in each single indentation was equal to the corresponding recorded impact peak force, which followed the principle as shown in Eq. (2). Furthermore, the RE-QSI and RF-QSI were both in displacement control; for the RF-QSI, each indentation was loaded until the indentation force reached the predefined value, which was determined with the impact peak force variation, and then the unloading phase began, whereas the RE-QSI started unloading as the expected indentation energy of 6.5 J was reached.

3.5. Damage detection

Whether a method used to correlate impacts and quasi-static indentations is appropriate depends on how the equivalence in damage is defined, and thus on the damage detection methods adopted.^{27,38,39} To thoroughly characterize the final damage statuses of the impacted and indented specimens, a combination of several non-destructive and destructive damage detection techniques was adopted. In order to characterize the surface damage features, the damaged surfaces of the impacted and indented specimens were scanned using a KEYENCE VR-5000 wide area 3D surface measurement machine (see Fig. 4(a)). Subsequently, all specimens were ultrasonically C-scanned so that projected damage areas could be obtained, the ultrasonic C-scan device is shown in Fig. 4(b). Afterwards, the damaged specimens were sectioned along the path as shown in Fig. 4(c) with an E281 secotom 10 precision cutting machine. The exposed cut surfaces were ground sequentially with 82, 46.2, 18, 8, and 5 μ m grit sandpapers and polished with diamond pastes. At last, the prepared samples were observed under a KEYENCE camera microscope (see Fig. 4(d)) at 5 \times magnification, with which the damage images of the entire exposed cross-sectional surfaces could be obtained by stitching the small micrographs of different local damage areas. The cross-sectional damage images were then replicated through Auto CAD 2020 software to facilitate comparisons between the internal impact and indentation damages.

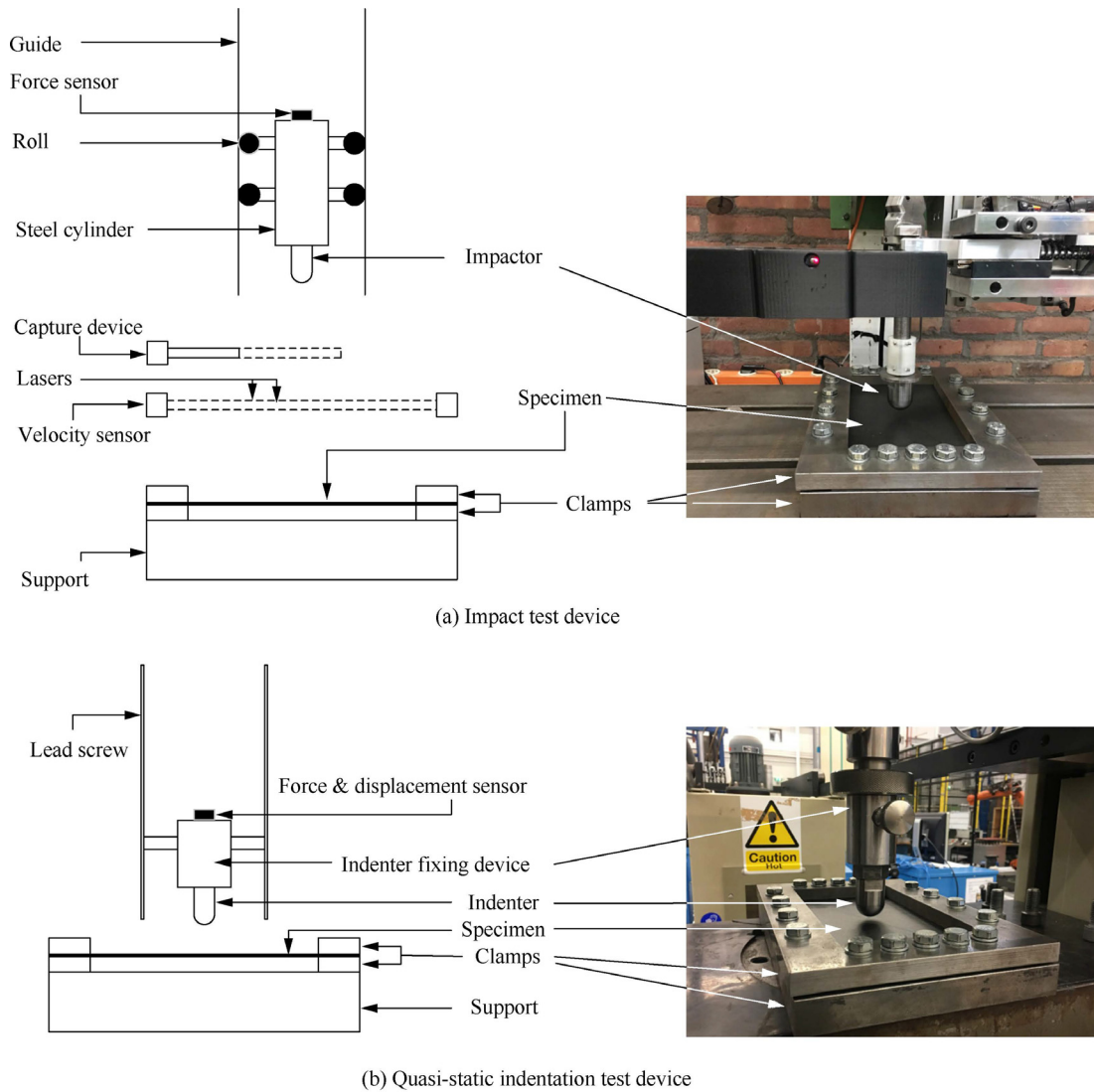


Fig. 3 Details of impact and quasi-static indentation test devices.

4. Results

4.1. Comparison of the plate responses

4.1.1. Force-displacement curves

Plate responses of a composite laminate subjected to out-of-plane impact/indentation loading are important for the formation of various damages. In general, similar plate responses imply that similar stress fields in a composite laminate undergoing different impact/indentation events can be induced, which could result in comparable final macroscopic damage statuses in term of strenght of materials. In addition, the responses of an impacted/indented composite laminate refer to its deformation behaviours under out-of-plane impact/indentation loading, which can be characterized by the recorded force-displacement curve, also known as force-deflection curve. To compare the plate responses of the repeatedly impacted and indented composite laminates, in this section, the 225 force-displacement curves for the RI, RE-QSI, and RF-QSI specimens during the loading and unloading stages

are compared, and these comparisons are summarized in Fig. 5.

Fig. 5(a) shows that all indentation force-displacement curves of the RE-QSI and RF-QSI specimens coincide well with those of the RI ones during the loading stages, though significant oscillations are found in those stages of the RI force-displacement curves. These oscillations in the impact force-displacement curves were caused by the propagation of flexural elastic waves associated with impacts, according to Minak and Ghelli,⁴⁰ which did not occur during the quasi-static indentations. Fig. 5(a) also shows that non-linear characteristics were inherent to all curves of the impacted and indented composite specimens. Kwon and Sankar⁴¹ reported that the nonlinearity in the initial portion of the force-displacement curves was attributed to the local Hertzian contact deformation, whereas the membrane effect induced by large deflection contributed to the subsequent nonlinearity. Besides, another distinguishable feature of the RE-QSI and RF-QSI curves during the loading phase was the change in the curve curvature (see Fig. 5(a)), which was essentially a reflection of

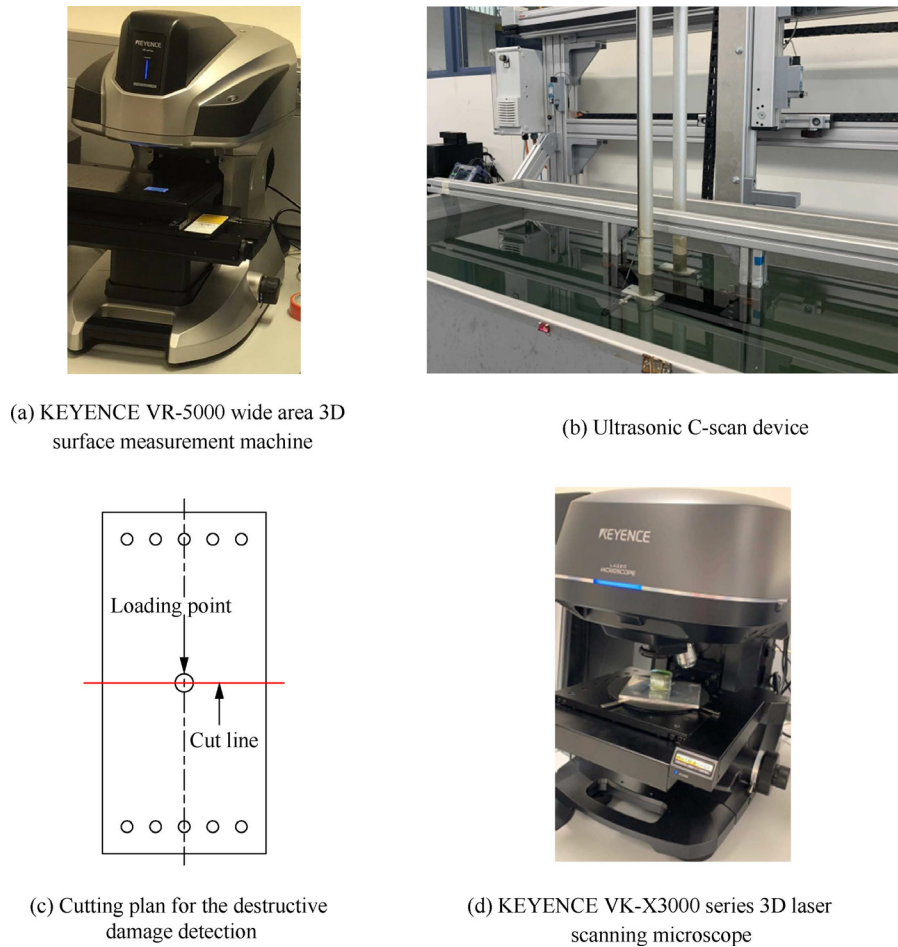


Fig. 4 Damage detection setups and specimen cutting plan.

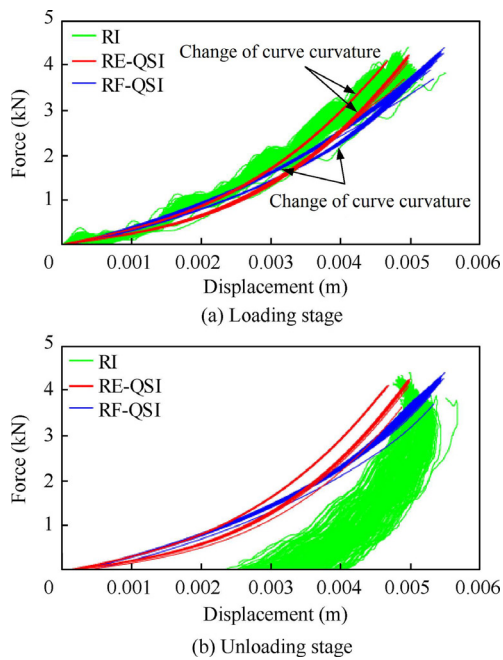


Fig. 5 Comparison of 225 force-displacement curves between RI, RE-QSI, and RF-QSI specimens.

sudden structural stiffness changes of the target laminate.³⁶ Furthermore, before and after the curvature variations, the force-displacement curves of the RE-QSI and RF-QSI specimens almost followed identical loading paths until peak forces were reached. In contrast, no such curvature changes were observed in the RI force-displacement curves, and the curves of different single impacts did not exactly coincide like their quasi-static counterparts.

For comparisons of the unloading phases, Fig. 5(b) shows that both of the RF-QSI and RE-QSI curves deviate greatly from the RI curves, and a similar observation was also reported by Nettles and Douglas.²² The unloading-phase RI curves have a larger hysteresis than those of the corresponding RF-QSI and RE-QSI curves, which indicates that more energy was involved during the unloading phase of an impact than in the indentation unloading stage. Moreover, Fig. 5(b) demonstrates another significant difference between the repeated impact and indentation force-displacement curves: the residual deformations of the indented laminates are much smaller than those of the impacted laminates. The residual deformation of an indented specimen was negligible when each indentation cycle was completed; however, the residual deformations of the impacted laminates varied between 2 to 4 mm. In this study, the inertial effect of a composite laminate is considered to be the underlying cause for such significant differences in

the residual deformations of the repeatedly impacted and indented cases, as discussed below.

Owing to the influence of the inertia of the plate during an impact, when the velocity of the impactor just reduced to zero (the impactor still contacted with the laminate at this moment), materials within the contact area and its adjacent regions still moved along their original directions. Therefore, as illustrated in Fig. 6(a), as the contact force became zero after a very short time interval of that instant, the impacted specimen was still in a significant deformation state, which led to the evident residual deformations of the RI specimen. However, such an inertial effect did not occur throughout the whole indentation process, and the indenter remained in contact with the specimen until the end of the indentation, which is illustrated in Fig. 6(b). Additionally, the residual deformation within the contact area of the impacted plate was a combination of the permanent surface dent (plastic deformation of the matrix) and plate deflection. The depth of the impact dent can be neglected compared to the significant residual impact deflection. In contrast, for the indented specimens, the only residual deformation was the indentation permanent dent. This resulted in that the indentation force–displacement curves could not exactly return back to zero when the indentation force just vanished.

To clearly demonstrate the discrepancies in plate responses of the impacted and indented composite laminates conveyed from the force–displacement curves, the 1st force–displacement curves of the RF-QSI and RI specimens were compared. The comparison is shown in Fig. 7, and the corresponding residual deformation features at the moment when the indentation/impact was just completed were also marked in this figure. For the indented composite specimens, as shown in Fig. 7, the peak force and displacement are coincident, but the impact peak displacement (D_{\max}) lags behind the impact peak force (F_{\max}). To highlight this difference, the displacement of the impacted specimens related to F_{\max} is denoted as $D_{F\max}$; the contact force corresponding to D_{\max} on the impact curve is represented by $F_{D\max}$.

The phenomenon of the peak impact displacement lagging behind the impact peak force was caused by the high impact loading rate. As a matter of fact, the impact contact force

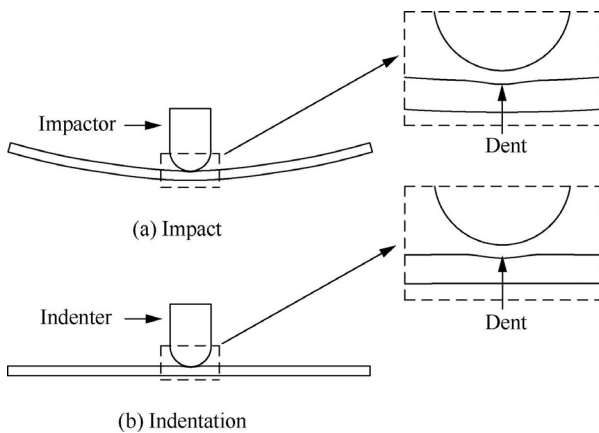


Fig. 6 Illustration of deformation state of laminates at the moment when impactor or indenter just lost contact with specimens.

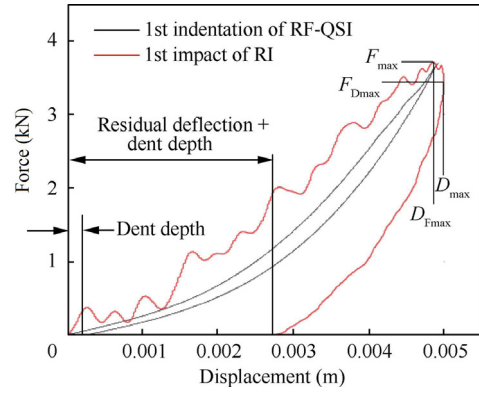


Fig. 7 Comparison of the 1st force–displacement curves between RF-QSI and RI specimens and their basic features.

was generated immediately at the instant when the impactor just touched the laminate, and then the corresponding materials started to move under the driving of this contact force. This finally translated into the impact peak force always preceding the impact peak displacement. On the contrary, the almost zero loading rate of the quasi-static indentation caused no such maximum contact force and maximum displacement out-of-phase phenomenon, as can be observed in the indentation force–displacement curves.

4.1.2. Peak force variations

The peak force in a force–displacement curve has been employed by several researchers to rank the impact load-carrying capabilities of various single impacted composite laminates.^{31–33} In this section, to further demonstrate the similarities and differences in the plate responses of the impacted and indented composite laminates, the variations of the peak forces with indentation/impact numbers are compared. Considering that the peak forces of the RF-QSI have exactly the same scatter as those of the RI (see the impact and indentation peak force relationships shown in Eq. (2)), here only the variations of the RE-QSI and RI peak forces are compared. The peak force variations with impact/indentation numbers are shown in Fig. 8. Because each indentation of the RE-QSI has an identical indentation energy of 6.51 J and each impact of the RI has the same impact energy of 8.45 J, the large scatter of the impact peak force variation indicates a weaker one-to-one correlation between the impact peak force and impact energy than

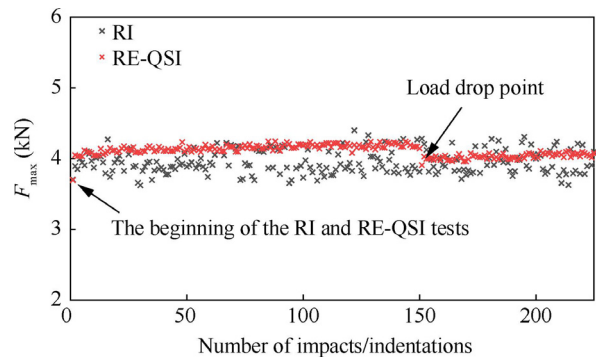


Fig. 8 Peak force variations of RE-QSI and RI specimens.

that in the indentation case. The scattered variation of the impact peak force could mainly result from the dynamic vibrations caused by the high impact loading rate, because the RE-QSI peak forces varied stably, and no dynamic vibrations presented during the entire indentation processes.

Moreover, Fig. 8 shows that, for the 2nd indentation of the RE-QSI and the 2nd impact of the RI tests, the peak forces increased for both cases compared to those of the corresponding 1st indentation and impact, which was due to resin hardening in the contact area caused by the contact force.²² The compacted contact area had a higher contact stiffness compared to that of its original state, which resulted in an increase in the peak force as the composite was subjected to another identical indentation or impact. After the 2nd indentation, the indentation peak forces stayed at a steady value until the 150th indentation, at which a drop in the peak force variation was observed. This force drop was potentially induced by a sudden change in the structural stiffness of the indented laminate due to an accumulation of damages.³⁶ In general, it is predominantly matrix cracking and delamination contributing to stiffness degradations in a composite laminate until extensive fibre breakage occurs,⁴² at which point the structure totally loses its load-carrying capability. After the load drop, the indentation peak forces re-stabilized at a smaller value. For the impact peak forces, however, they always varied randomly between 3600 and 4250 N until all 225 impacts were completed. Meanwhile, the upper bound of the impact peak force variation before the 150th impact was close to the stable indentation peak forces. After the force drop, the impact peak forces were observed to be evenly distributed in the areas adjacent to the indentation peak forces.

In summary, the loading rate and inertial effect could bring significant discrepancies in the plate responses of impacted and indented composite laminates. A high impact loading rate introduced dynamic vibration into the impact system (i.e., the combination of the impact device and impact target), which in turn resulted in vibrations in the impact force–displacement curve and large scatter in the impact peak force variation. A high loading rate also caused the impact contact force to always proceed the corresponding displacement, while the plate inertial effect induced significant residual deformation at the instant as the impactor and specimen just lost contact. As for the abilities of those two quasi-static approaches to reproduce repeated impact responses, the RF-QSI method could accurately track the variation of impact peak forces, whereas the RE-QSI force–displacement curves fitted the RI curves better than the RF-QSI ones during the loading stages. However, neither of them could produce similar force–displacement curves to those of the RI specimens during the unloading stage, due to that both of these two quasi-static methods failed to simulate the inertial effect that was usually accompanied by a high impact loading rate.

4.2. Comparison of damage behaviours

CFRP composites are typical brittle materials, which means that macroscopically only elastic and damage phases can be distinguished during an impact or indentation process. Those above comparisons are limited to the elastic plate responses of repeatedly impacted and indented composite laminates. For the purpose of understanding the similarities and differ-

ences in damage behaviours, and to determine which quasi-static method is more feasible in mimicking impact damage behaviours, the damage morphologies of different composite specimens were compared in this section.

4.2.1. Surface damage morphology comparison

Firstly, the surface damages within and around the contact areas of repeatedly indented and impacted specimens were compared. For this, the tested specimens were scanned under a KEYENCE VR-5000 wide area 3D surface measurement machine. Using this machine, the 2D and 3D surface damage morphologies could be obtained directly, which are shown in Figs. 9 and 10, respectively. Fig. 9 shows that the 2D damaged surfaces of the RI, RF-QSI, and RE-QSI specimens have very similar damage characteristics: no matrix failures were observed within the contact areas. Instead, there are two straight surface cracks that coincide with the diameter of the contact area and along the -45° fibre direction, which indicates that these surface cracks grew perpendicular to the indented/impacted surface fibre orientation.

In addition, the 3D surface damage morphologies shown in Fig. 10 clearly illustrate the major difference between the repeatedly impacted and indented specimens, i.e., the maximum indentation dent depth is deeper than the maximum dent depth of its impact counterpart (about 3 and 0.6 μm for the impacted and indented cases, respectively). Contrastingly, the in-plane diameter (i.e., the dent diameter that is contained in the impacted/indented surface of the specimen) of the impact dent is approximately 10 mm and is close to that of the indentation dent (~ 9 mm). Because the permanent impact/indentation dent is essentially the result of plastic deformation of the matrix directly induced by contact force/pressure, strain rate hardening of the polymer matrix is considered to be the major reason for such discrepancy in maximum dent depths of the impacted and indented composite specimens. As a matter of fact, the loading rates of the investigated repeated impacts were several thousand times larger than those of the quasi-static indentations, given that the single impact duration in this study was about 0.006 s, while the entire single indentation process took about 2 min.

4.2.2. Surface damage morphology comparison

Due to the opaque nature of the CFRP laminate, it is impossible to directly observe internal damages without the assistance of damage detection techniques. For the purpose of obtaining a basic understanding about the internal damages of the impacted and indented composite laminates, the features of the recorded C-scan damages were first evaluated, and the corresponding C-scan recordings are shown in Fig. 11. Fig. 11 shows that the biggest difference between the impact and indentation C-scan damages is that no damages were observed in the centre of the indentation C-scan damage areas (labelled I in Fig. 11(a) and (c)). These undamaged areas were high out-of-plane compression and low out-of-plane shear stress areas, as the maximum indentation forces were just reached.⁴³

In general, a high out-of-plane compression stress prevents propagation of delaminations in indented/impacted composite laminate, while high out-of-plane shear stresses induce the initiation of matrix cracks that trigger the onset of delamination, and the out-of-plane shear stresses are also believed to be the

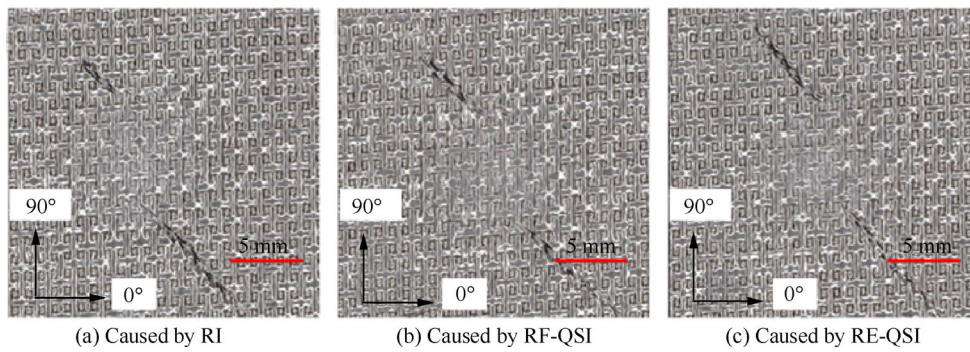


Fig. 9 Two-dimensional surface damage morphologies caused by different repeated out-of-plane concentrated loads; note that RI consisted of 225 impacts and both RF-QSI and RE-QSI consisted of 225 indentations.

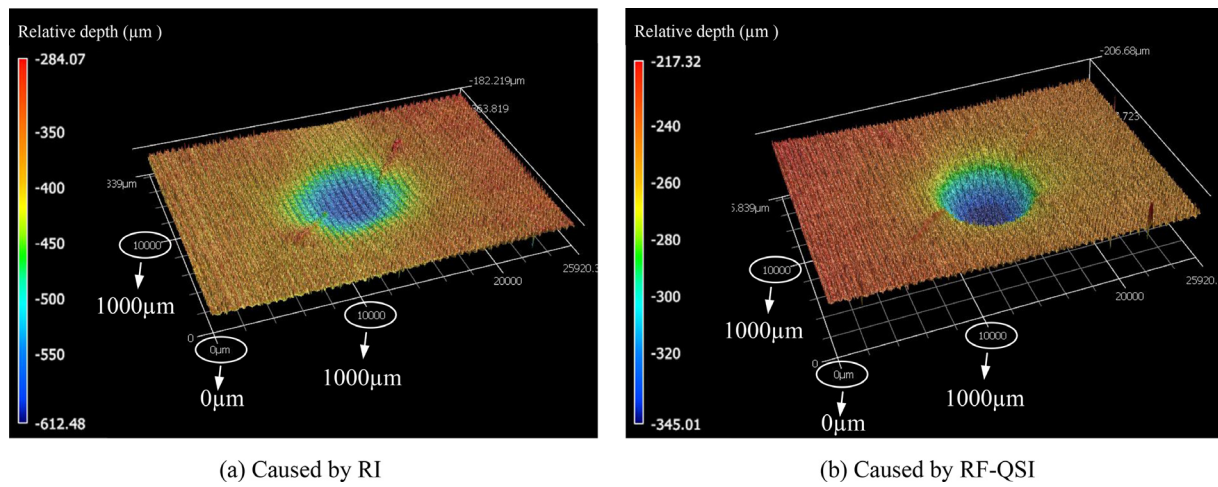


Fig. 10 Three-dimensional surface damage morphologies; note that the RI and RE-QSI consisted of 225 impacts and 225 indentations, respectively.

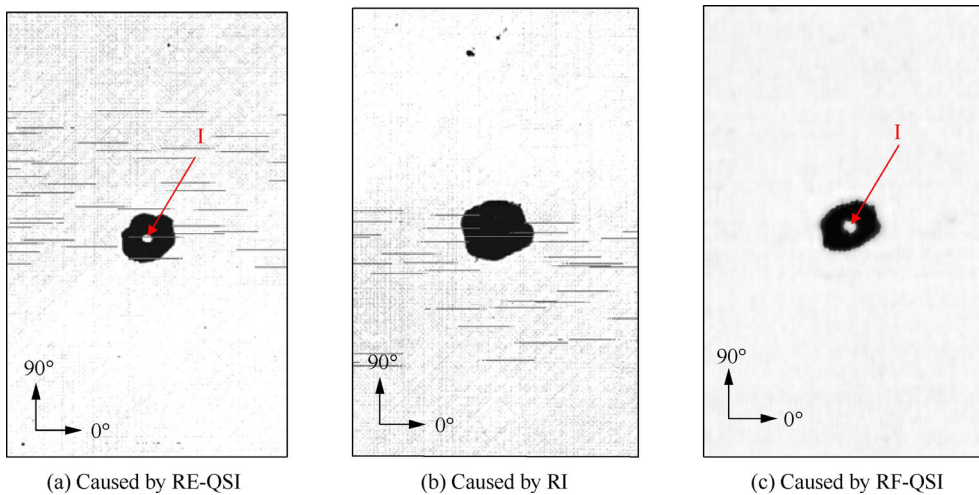


Fig. 11 Projected ultrasonic C-scan damage areas; note that RI consisted of 225 impacts, and both RF-QSI and RE-QSI consisted of 225 indentations.

major forces driving the subsequent delamination propagation. Further, literature has shown that, for a transversely indented composite laminate, an out-of-plane compression stress is induced by the contact pressure, and out-of-plane shear stresses are caused by a combination of local contact and global bending deformations.⁴⁴

In this study, it was observed that the indenter remained in contact with the specimen throughout the whole indentation process. Therefore, for the quasi-static indentations, the out-of-plane compression and shear stresses always occurred simultaneously within the contact area and caused the indentation delaminations to fail to propagate in the contact centre region. However, for the impacts, from the instant when the rebound of the impactor began to the loss of contact between the impactor and specimen, the out-of-plane compression stress gradually disappeared from the contact area. Meanwhile, as shown in Fig. 5(b) and illustrated in Fig. 6(a), the impacted specimen was still significantly deformed. This resulted in the out-of-plane shear and compression stresses being out-of-phase during this very short time interval after the impactor rebound just began, so that the formed impact delaminations could propagate within the contact area.

To compare the projected C-scan damages of the RI, RE-QSI, and RF-QSI specimens more intuitively, the damage envelopes were obtained through the AutoCAD 2020 software and compared in the same polar coordinate system, which are shown in Fig. 12. The comparisons show that the RI specimen has a roughly circular damage shape, while those of the RE-QSI and RF-QSI specimens are close to ellipses with their major axes parallel to the 45° direction. Moreover, the RI specimen has the largest C-scan damage area among all cases, and the C-scan damage envelop of the RE-QSI specimen is closer to that of the RI specimen than the RF-QSI one, owing to the RE-QSI and RI specimens have similar C-scan damage envelop diameter lengths along the 45° direction. However, neither the RF-QSI nor the RE-QSI methods could induce exactly the same C-scan damage area shape as that of the RI method in the composite laminates.

Because the RF-QSI and RE-QSI specimens have almost elliptical C-scan damages, whereas that of the RI specimen is

almost circular, the factors affecting the formation of damages of the repeatedly impacted and indented composite laminates should be different. Besides, the C-scan damage is usually a superposition of several single delaminations at different ply interfaces, and the discrepancy between the impact and indentation C-scan damages is therefore essentially a reflection of the difference between the formed impact and indentation delaminations. Fig. 12 shows that the magnitude of the difference between the impacted and indented delaminations depends on the direction; moreover, it is known that the propagation speed of the impact-induced flexural elastic wave is also direction-dependent.⁴⁵ Therefore, the underlying reason for the discrepancy between the impact and indentation C-scan damages should be most relevant to the effect of the flexural wave on the delamination growth. However, a detailed justification of this statement is not given in this study considering the complexity of the potential problem(s); instead, it can be proposed as a hypothesis for further studies. Furthermore, owing to that both the RF-QSI and RE-QSI methods induced smaller projected delamination areas compared to those of the repeated impacts, in terms of the delaminations formed, it is conservative to use the repeated quasi-static indentations to approximate the repeated impacts.

4.2.3. Cross-sectional damage comparison

The surface and C-scan damages lack details on through-thickness damage distributions, to overcome this problem, the tested RI, RF-QSI, and RE-QSI specimens were sectioned along the red line shown in Fig. 4(c). The relevant cross-sectional damage morphologies are summarised in Fig. 13, which shows that all specimens have similar delamination distributions, most of the single delaminations are symmetrical around the centrelines of the samples (red dashed lines in Fig. 13), and the longest delaminations were observed at the interfaces adjacent to the mid-planes of the laminates. Those similar delamination distributions indicate that the delaminations in the impacted and indented laminates in the cut direction follow similar growth principles. The basic feature of the damages obtained by C-scan can also be highlighted by the detailed cross-sectional damages. It was observed from the C-scan results that no damage was detected within the contact centres of the RF-QSI and RE-QSI specimens (see Fig. 11), and the internal damage statuses of these regions with no detectable C-scan damages can be provided by the cross-sectional damages. As shown in Fig. 13, delaminations also exist in these undamaged regions in the C-scan results of the RF-QSI and RE-QSI specimens, but the delamination densities within those areas are negligibly small compared to that of the impact one, especially in the RF-QSI case. Additionally, the low-delamination density area has a cone shape, which is shown in Fig. 13(b)(iii).

Two types of matrix cracks are shown in Fig. 13: one is connected with and formed part of the delamination (see the short blue lines), and the other is independent of the delamination (see the cyan lines). The cracks associated with the impact and indentation delaminations all typically have an approximate 45° inclination, which suggests that these cracks were caused by the out-of-plane shear stresses. For an impacted composite laminate, the delaminations are always induced by these inclined matrix cracks.⁴⁶ The similarities between the indentation and impact matrix cracks, which are connected

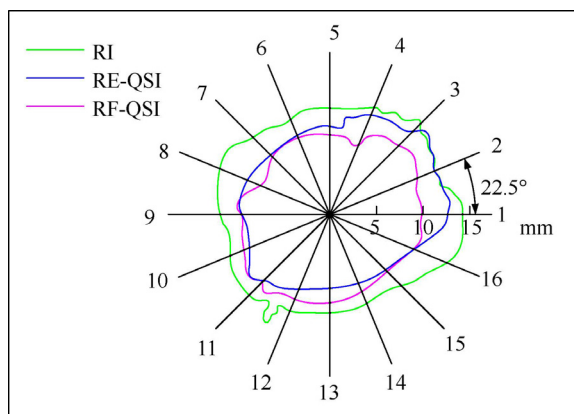
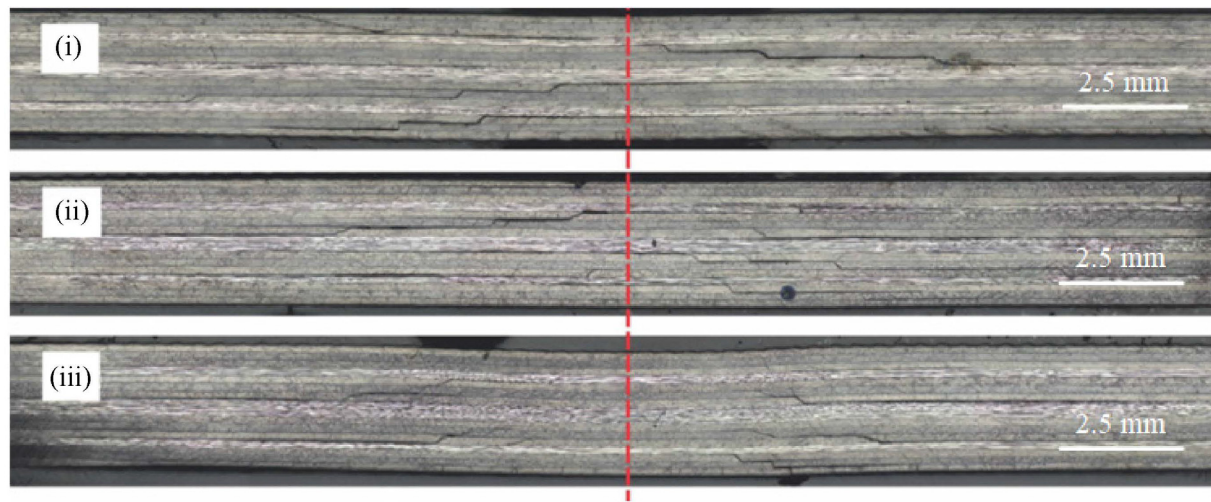


Fig. 12 Comparison of C-scan damage envelopes between RI, RE-QSI, and RF-QSI specimens; note that RI consisted of 225 impacts, and both RF-QSI and RE-QSI consisted of 225 indentations.



(a) Original cross-sectional damage morphologies

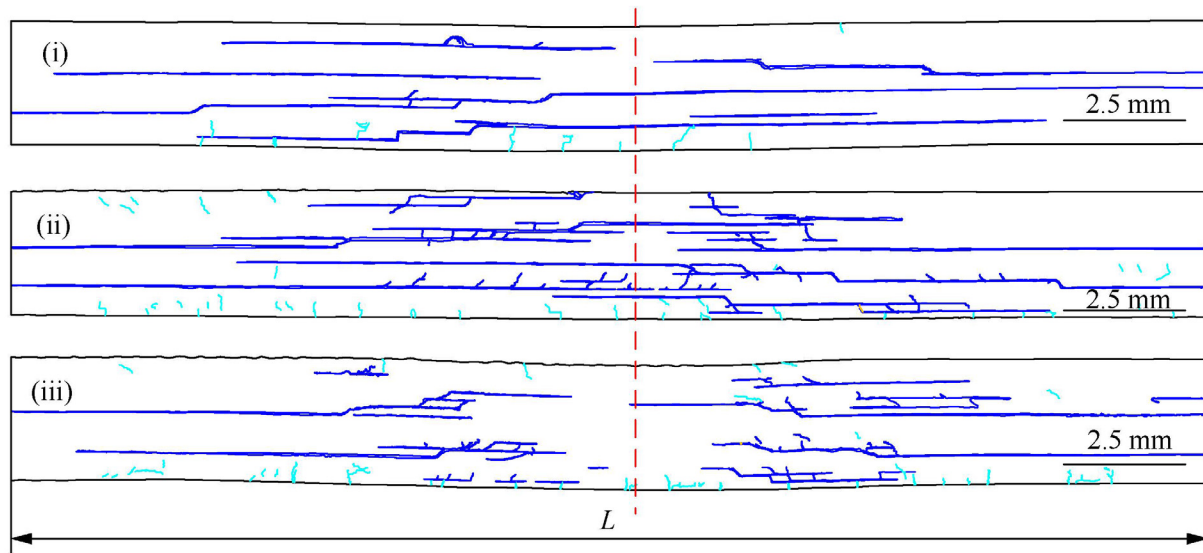
(b) Processed cross-sectional damage morphologies (delaminations and their associated matrix cracks are represented by the blue lines; the isolated matrix cracks are represented by the cyan lines), where L refers to the length of the rectangular cross-section.

Fig. 13 Cross-sectional damage morphologies of the specimens: (i) caused by the RE-QSI, (ii) caused by the RI, and (iii) caused by the RF-QSI; note that the RI consisted of 225 impacts, and both the RF-QSI and RE-QSI consisted of 225 indentations.

to the delaminations, indicate similar delamination initiation mechanisms between the impact and indentation cases. Fig. 13 also shows that the impacted specimen has the densest matrix cracks that are linked to the delaminations, and the matrix crack and delamination distributions of the RF-QSI specimen are more similar to those of the RI specimen if the damages just beneath the impact site are not taken into account. As for the isolated matrix cracks, most of them are distributed vertically near the bottom sides of the specimens and are symmetrical about the centrelines of the samples. Those isolated matrix cracks are believed to be caused by the in-plane tensile stresses. Besides, the isolated matrix cracks of

these three specimens are very close to each other in both distribution and density, which emphasizes that the in-plane tensile stress distributions induced by laminate bending deformations are less dependent on the potential impact-related damage formation influencing factors. Note that the fibre failures of the repeatedly impacted and indented composite laminates were not compared in this study. The reason is that the majority of fibre failures (i.e., fibre compressive and tensile failures) were generally removed from the cross-sections when polishing the microscopic samples, and the remaining fibre failures were hidden inside the matrix cracks and delaminations. This means that the major damage features

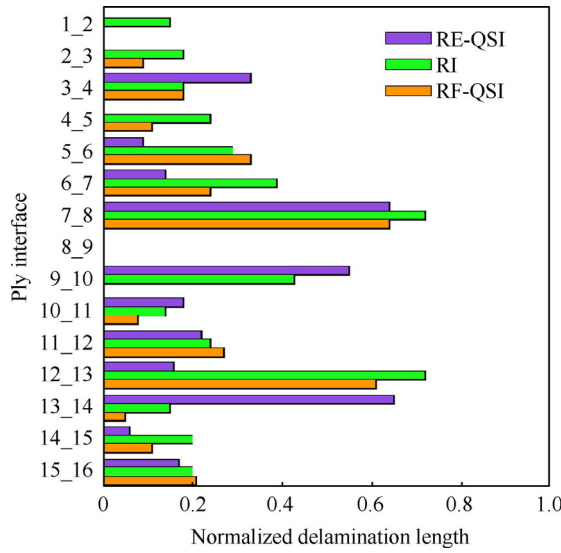


Fig. 14 Comparison of normalized single delamination lengths at different ply interfaces of different specimens.

of the fibre failures were either destroyed or hidden, which in turn renders the comparisons of the impact and indentation fibre failures meaningless.

In general, comparing quantified damages is a more reasonable way to convey differences among various damage modes associated with different loading conditions than directly comparing the corresponding damage morphologies. Delamination is a damage mode that is easier to be observed and quantified than matrix cracks and fibre breakage and can thus be adopted as a similarity indicator between the repeated impacts and repeated quasi-static indentations damage behaviours. To quantify the comparison of the impact and indentation delaminations, the lengths of the single delaminations at different ply interfaces were measured. These single delamination lengths were then normalized by the lengths of the rectangular cross-sections (labelled L in Fig. 13(b)(iii)), and the normalized delamination lengths of different ply interfaces are finally presented in Fig. 14. This detailed ply-by-ply normalized delamination length comparison suggests that the delaminated

interface amounts of the impacted and indented specimens are broadly similar, but no indentation delamination was observed at the interface 1_2.

Further, based on the data shown in Fig. 14, the absolute differences between the normalized impact and indentation delamination lengths at different ply interfaces, $D_{n, \text{RE-QSI}}$ and $D_{n, \text{RF-QSI}}$, can be calculated as

$$D_{n, \text{RE-QSI/RF-QSI}} = |L_{n, \text{RI}} - L_{n, \text{RE-QSI/RF-QSI}}| \quad (4)$$

where n refers to the n^{th} ply interface, and the 1st one is that closest to the impact/indentation surface. $L_{n, \text{RI}}$, $L_{n, \text{RE-QSI}}$, and $L_{n, \text{RF-QSI}}$ are the normalized cross-sectional delamination lengths at the n^{th} ply interface of the RI, RE-QSI, and RF-QSI specimens, respectively. Therefore, the parameters $D_{n, \text{RE-QSI}}$ and $D_{n, \text{RF-QSI}}$ can be used to evaluate the capability of the RE-QSI and RF-QSI methods in mimicking the impact delamination behaviours, and according to their definitions in Eq. (4), the smaller $D_{n, \text{RE-QSI}}$ or $D_{n, \text{RF-QSI}}$ is, the better the similarity between the impact and indentation delaminations is.

The specific values for $D_{n, \text{RE-QSI}}$ and $D_{n, \text{RF-QSI}}$ are tabulated in Table 1, with which three different cases, i.e., $D_{n, \text{RE-QSI}} > D_{n, \text{RF-QSI}}$, $D_{n, \text{RE-QSI}} = D_{n, \text{RF-QSI}}$, and $D_{n, \text{RE-QSI}} < D_{n, \text{RF-QSI}}$, can be distinguished. Table 1 shows that the percentage of $D_{n, \text{RE-QSI}} > D_{n, \text{RF-QSI}}$ is 53.33% (where $n = 3, 5, 9, 10, 11, 12, 13, 15$), whereas in the case of $D_{n, \text{RE-QSI}} < D_{n, \text{RF-QSI}}$ (where $n = 1, 4, 6, 7, 14$), the percentage is 33.33%. This indicates that the single delamination lengths at different ply interfaces induced by the RF-QSI method are closer to the RI loading condition.

5. Discussion

This work proposed an automated quasi-static test procedure to mimic the repeated impact response and damage behaviour of CFRP composite laminates and compared it with another newly developed semi-automatic quasi-static solution. Their abilities in mimicking the repeated impact response and damage behaviour were evaluated in terms of the similarities in plate responses and final damage state. Based on the investigation outputs, the impact-mimicking performances with regard to plate responses and damages of the RE-QSI and RF-QSI methods as well as their automations are illustrated in Fig. 15.

5.1. Plate response

Loading rate and inertial effect are the two major factors that contribute to the gap between the plate responses (represented by the force–displacement curve and peak force variation) of the

Table 1 Specific values for $D_{n, \text{RE-QSI}}$ and $D_{n, \text{RF-QSI}}$ at different ply interfaces.

Ply interface	$D_{n, \text{RE-QSI}}$	$D_{n, \text{RF-QSI}}$	$D_{n, \text{RE-QSI}} - D_{n, \text{RF-QSI}}$
1_2 ($n = 1$)	0.00	0.15	−0.15
2_3 ($n = 2$)	0.09	0.09	0.00
3_4 ($n = 3$)	0.15	0.00	0.15
4_5 ($n = 4$)	0.11	0.13	−0.02
5_6 ($n = 5$)	0.24	0.04	0.20
6_7 ($n = 6$)	0.10	0.15	−0.05
7_8 ($n = 7$)	0.00	0.08	−0.08
8_9 ($n = 8$)	0.00	0.00	0.00
9_10 ($n = 9$)	0.55	0.43	0.12
10_11 ($n = 10$)	0.10	0.06	0.04
11_12 ($n = 11$)	0.05	0.03	0.02
12_13 ($n = 12$)	0.45	0.11	0.34
13_14 ($n = 13$)	0.60	0.10	0.50
14_15 ($n = 14$)	0.05	0.09	−0.04
15_16 ($n = 15$)	0.04	0.01	0.03

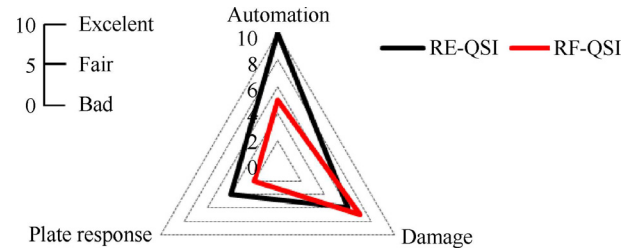


Fig. 15 Illustration of the performances for the two quasi-static solutions to mimic the repeated impact response and damage behaviour of CFRP laminates.

repeatedly impacted and repeatedly indented composite laminates. The dynamic vibration associated with a high impact loading rate induced evident noise in the recorded impact force–displacement curves (Fig. 5) and large scatter in the peak impact force variation (Fig. 8). The high loading rate also directly caused the contact forces to precede the corresponding material displacements. In particular, as shown in Fig. 7, it resulted in the impact peak displacement lagging behind the peak forces. Moreover, the significant residual deformation associated with the inertial effect at the moment when the impactor and specimen just lost contact was observed, which did not occur in the indentation process. Because the loading rate of the quasi-static indentation is quite small compared to that of the impact and the inertial effect for the indented composite laminates is negligible, the indentation contact force and the material displacement were always present simultaneously during the entire indentation process. These comparisons showed that both the RF-QSI and RE-QSI methods failed to imitate impact plate responses which were highly affected by the loading rate and inertial effect. However, Fig. 5(a) showed that the loading phases of the impact and indentation force–displacement curves were comparable, which indicated that the loading phase of the impact curve was less dependent on the loading rate and inertial effect, and the RE-QSI curves fit the repeated impact curves better than those of the RF-QSI. Though neither mimic reproduced impact plate responses well, the RE-QSI outperformed the RF-QSI.

5.2. Damage

Compared to the final repeated impact damage state, both the RE-QSI and RF-QSI methods induced quite similar surface damages (i.e., permanent dent and surface crack, as shown in Fig. 9), comparable projected delamination areas (Fig. 11), similar internal damage distributions (i.e., matrix crack and delamination distributions, as shown in Fig. 13), and similar delamination lengths at different ply interfaces (Fig. 14). These similar impact and indentation damage morphologies demonstrated that the damage mechanisms for the repeatedly impacted and indented composite laminates were rather close to each other.

However, there were also different features between the impact and indentation damages, such as the shallower impact dent depth compared to that of the indentation case (Fig. 10), and no damages in the centre of the projected indentation delamination area (Fig. 11). The shallower maximum impact dent depth could be attributed to the strain rate hardening effect of the matrix, and the contact between the impactor and the laminate that ended prematurely relative to the significant impact deformations was responsible for the formation of delaminations in the contact area centre. Owing to that the RF-QSI method induced a closer matrix crack distribution (Fig. 13) and closer normalized cross-sectional delamination lengths (Table 1) to those of the impact cases than those associated with the RE-QSI method, the RF-QSI has better impact damage reproducibility than that of the RE-QSI, which is illustrated in Fig. 15.

5.3. Automation

The RF-QSI method was performed in a semi-automatic fashion, as for each indentation of the RF-QSI, the indentation

peak force needed to be manually adjusted according to the recorded impact peak force variation. After that, each indentation of the RF-QSI could be performed automatically. On the contrary, for the RE-QSI, owing to that the indentation energy was the same for all single indentations, once the indentation energy and total number of indentations were input into the control system of the testing machine, the RE-QSI could be conducted in a completely automatic way like mechanical fatigue testing. Therefore, in terms of degree of automation, the RE-QSI method has an inherent advantage over the RF-QSI one.

6. Conclusions

The capabilities of two quasi-static approaches to mimic repeated impact response and damage behaviour of multidirectional CFRP composite laminates were investigated. The similarities between the indentation and impact behaviours were evaluated through comparisons of the plate responses (represented by the force–displacement curve and peak force variation) and final damage status (i.e., surface damage, projected delamination area, cross-sectional delamination, and matrix crack distribution). The main conclusions are:

- High loading rate and inertial effect are the two major factors affecting the responses of repeatedly impacted composite laminates. The high impact loading rate induced serious vibrations in the impact system and caused the contact forces to always lead the related material displacements, while the inertial effect resulted in significant residual plate deformation at the instant when the impactor and composite laminate just lost contact. Both the RE-QSI and RF-QSI methods failed to mimic the impact responses that were highly influenced by these two factors.
- The RF-QSI method can yield better similarities in the final repeated impact damage state of composite laminates than those of the RE-QSI method. However, the RE-QSI can be automated and has better reproducibility of the repeated impact responses, which are less dependent on the loading rate and inertial effect, whereas the RF-QSI cannot be performed in such an automatic fashion, as the input peak indentation forces must be adjusted each time to follow the varied impact peak force recordings.

Declaration of Competing Interest

The authors declare that they have no known competing financial interests or personal relationships that could have appeared to influence the work reported in this paper.

Acknowledgement

The authors gratefully acknowledge the financial support from the China Scholarship Council (No. CSC201806290014).

References

1. Tang CS, Zimmerman JD, Nelson JI. Managing new product development and supply chain risks: the Boeing 787 case. *Supply Chain Forum Int J* 2009;10(2):74–86.

2. Herzog D, Schmidt-Lehr M, Canisius M, et al. Laser cutting of carbon fiber reinforced plastic using a 30 kW fiber laser. *J Laser Appl* 2015;**27**(S2):S28001.
3. Lewis SJ. The use of carbon fibre composites on military aircraft. *Compos Manuf* 1994;**5**(2):95–103.
4. Kreculj D, Rašuo B. Review of impact damages modelling in laminated composite aircraft structures. *Tehnicki Vjesnik Tech Gazette* 2013;**20**:485–95.
5. Davies GAO, Zhang X. Impact damage prediction in carbon composite structures. *Int J Impact Eng* 1995;**16**(1):149–70.
6. Davies GAO, Olsson R. Impact on composite structures. *Aeronaut J* 2004;**108**(1089):541–63.
7. Elder DJ, Thomson RS, Nguyen MQ, et al. Review of delamination predictive methods for low speed impact of composite laminates. *Compos Struct* 2004;**66**(1–4):677–83.
8. Braem M, Lambrechts P, Van Doren V, et al. The impact of composite structure on its elastic response. *J Dent Res* 1986;**65**(5):648–53.
9. Cantwell WJ, Morton J. Comparison of the low and high velocity impact response of CFRP. *Composites* 1989;**20**(6):545–51.
10. Sevkai E, Liaw B, Delale F, et al. Effect of repeated impacts on the response of plain-woven hybrid composites. *Compos B Eng* 2010;**41**(5):403–13.
11. Zhou J, Wen P, Wang S. Numerical investigation on the repeated low-velocity impact behavior of composite laminates. *Compos B Eng* 2020;**185**:107771.
12. de Morais WA, Monteiro SN, d'Almeida JRM. Evaluation of repeated low energy impact damage in carbon-epoxy composite materials. *Compos Struct* 2005;**67**(3):307–15.
13. Wyrick DA, Adams DF. Residual strength of a carbon/epoxy composite material subjected to repeated impact. *J Compos Mater* 1988;**22**(8):749–65.
14. Winkel JD, Adams DF. Instrumented drop weight impact testing of cross-ply and fabric composites. *Composites* 1985;**16**(4):268–78.
15. Hufenbach W, Ibrahim FM, Langkamp A, et al. Charpy impact tests on composite structures – an experimental and numerical investigation. *Compos Sci Technol* 2008;**68**(12):2391–400.
16. Wagih A, Maimi P, Blanco N, et al. A quasi-static indentation test to elucidate the sequence of damage events in low velocity impacts on composite laminates. *Compos A Appl Sci Manuf* 2016;**82**:180–9.
17. Bull DJ, Spearing SM, Sinclair I. Investigation of the response to low velocity impact and quasi-static indentation loading of particle-toughened carbon-fibre composite materials. *Compos A Appl Sci Manuf* 2015;**74**:38–46.
18. Lagace PA, Williamson JE, Wilson Tsang PH, et al. A preliminary proposition for a test method to measure (impact) damage resistance. *J Reinf Plast Compos* 1993;**12**(5):584–601.
19. Weiridie BL, Lagace PA. On the use of quasi-static testing to assess impact damage resistance of composite shell structures. *Mech Compos Mater Struct* 1998;**5**(1):103–19.
20. Naik NK, Shirao P, Reddy BCK. Ballistic impact behaviour of woven fabric composites: formulation. *Int J Impact Eng* 2006;**32**(9):1521–52.
21. Kaczmarek H, Maison S. Comparative ultrasonic analysis of damage in CFRP under static indentation and low-velocity impact. *Compos Sci Technol* 1994;**51**(1):11–26.
22. Nettles AT, Douglas MJ. A comparison of quasi-static indentation to low-velocity impact. Huntsville:NASA Marshall Space Flight Center; 2000. Report No.:NASA/TP-2000-210481.
23. Lee SM, Zahuta P. Instrumented impact and static indentation of composites. *J Compos Mater* 1991;**25**(2):204–22.
24. Sjöblom PO, Hartness JT, Cordell TM. On low-velocity impact testing of composite materials. *J Compos Mater* 1988;**22**(1):30–52.
25. Symons DD. Characterisation of indentation damage in 0/90 lay-up T300/914 CFRP. *Compos Sci Technol* 2000;**60**(3):391–401.
26. Sutherland LS, Guedes SC. The use of quasi-static testing to obtain the low-velocity impact damage resistance of marine GRP laminates. *Compos B Eng* 2012;**43**(3):1459–67.
27. Castellano A, Fraddosio A, Piccioni MD. Quantitative analysis of QSI and LVI damage in GFRP unidirectional composite laminates by a new ultrasonic approach. *Compos B Eng* 2018;**151**:106–17.
28. Aoki Y, Suemasu H, Ishikawa T. Damage propagation in CFRP laminates subjected to low velocity impact and static indentation. *Adv Compos Mater* 2007;**16**(1):45–61.
29. Azwan SMS, Yazid YM, Amran A, et al. Quasi-static indentation behaviour of glass fibre reinforced polymer. *Adv Mater Res* 2014;**970**:317–9.
30. Lammerant L, Verpoest I. Modelling of the interaction between matrix cracks and delaminations during impact of composite plates. *Compos Sci Technol* 1996;**56**(10):1171–8.
31. Liu D. Characterization of impact properties and damage process of glass/epoxy composite laminates. *J Compos Mater* 2004;**38**(16):1425–42.
32. Zhou G. Static behaviour and damage of thick composite laminates. *Compos Struct* 1996;**36**(1–2):13–22.
33. Zhou G, Davies GAO. Impact response of thick glass fibre reinforced polyester laminates. *Int J Impact Eng* 1995;**16**(3):357–74.
34. Liu D, Raju BB, Dang X. Impact perforation resistance of laminated and assembled composite plates. *Int J Impact Eng* 2000;**24**(6–7):733–46.
35. Boukhili R, Bojji C, Gauvin R. Fatigue mechanisms under low energy repeated impact of composite laminates. *J Reinf Plast Compos* 1994;**13**(10):856–70.
36. ASTM. D6264/D6264M-17 Standard Test Method for Measuring the Damage Resistance of a Fiber-Reinforced Polymer-Matrix Composite to a Concentrated Quasi-Static Indentation Force. 2017:1–12.
37. ASTM. D7136/D7136M-20 Standard Test Method for Measurement the Damage Resistance of a Fiber-Reinforced Polymer Matrix Composite to a Drop-Weight Impact Event. 2020:1–16.
38. Asokkumar A, Jasiūnienė E, Raišutis R, et al. Comparison of ultrasonic non-contact air-coupled techniques for characterization of impact-type defects in pultruded GFRP composites. *Materials* 2021;**14**(5):1058.
39. Saeedifar M, Zarouchas D. Damage characterization of laminated composites using acoustic emission: a review. *Compos B Eng* 2020;**195**:108039.
40. Minak G, Ghelli D. Influence of diameter and boundary conditions on low velocity impact response of CFRP circular laminated plates. *Compos B Eng* 2008;**39**(6):962–72.
41. Kwon YS, Sankar BV. Indentation-flexure and low-velocity impact damage in graphite epoxy laminates. *J Compos Technol Res* 1993;**15**(2):101.
42. Shi Y, Pinna C, Soutis C. Modelling impact damage in composite laminates: a simulation of intra- and inter-laminar cracking. *Compos Struct* 2014;**114**:10–9.
43. Esrail F, Kassapoglou C. An efficient approach for damage quantification in quasi-isotropic composite laminates under low speed impact. *Compos B Eng* 2014;**61**:116–26.
44. Talagani MR. *Impact analysis of composite structures [dissertation]*. Delft: Delft University of Technology; 2014.
45. Fällström KE, Lindgren LE, Molin NE, et al. Transient bending waves in anisotropic plates studied by hologram interferometry. *Exp Mech* 1989;**29**(4):409–13.
46. de Moura MFSF, Marques AT. Prediction of low velocity impact damage in carbon-epoxy laminates. *Compos A Appl Sci Manuf* 2002;**33**(3):361–8.